

# A General Framework for Portfolio Construction Based on Generative Models of Asset Returns

Tuoyuan Cheng<sup>a,\*</sup>, Kan Chen<sup>a,b</sup>

<sup>a</sup>*Risk Management Institute, National University of Singapore, 04-03 Heng Mui Keng Terrace, 13 Building, Singapore, 119613, Singapore*

<sup>b</sup>*Department of Mathematics, National University of Singapore, Level 4, Block S17, 10 Lower Kent Ridge Road, Singapore, 119076, Singapore*

---

## Abstract

In this paper, we present an integrated approach to portfolio construction and optimization, leveraging high-performance computing capabilities. We first explore diverse pairings of generative model forecasts and objective functions used for portfolio optimization, which are evaluated using performance-attribution models based on least absolute shrinkage and selection operator (LASSO). We illustrate our approach using extensive simulations of cryptocurrency portfolios, and we show that the portfolios constructed using the vine-copula generative model and the Sharpe-ratio objective function consistently outperform. To accommodate a wide array of investment strategies, we further investigate portfolio blending and propose a general framework for evaluating and combining investment strategies. We employ an extension of the multi-armed bandit framework and use value models and policy models to construct eclectic blended portfolios based on past performance. We consider similarity and optimality measures for value models and employ probability-matching (“blending”) and a greedy algorithm (“switching”) for policy models. The eclectic portfolios are also evaluated using LASSO models. We show that the value model utilizing cosine similarity and logit optimality consistently delivers robust superior performances. The extent of outperformance by eclectic portfolios over their benchmarks significantly surpasses that achieved by individual generative model-based portfolios over their respective benchmarks.

*Keywords:* Portfolio construction, Generative model, Multi-armed bandit,

---

\*Corresponding author: tuoyuan.cheng@nus.edu.sg

## 1. Introduction

Since the seminal works of Markowitz, Finetti, and Roy seven decades ago, significant efforts from academia and industry have been devoted to portfolio theories (Markowitz, 1952, 1999, 2006; Roy, 1952; Rubinstein, 2002). The Mean-variance optimization (MVO) leverages the first and second moments of the portfolio return to establish a risk-return trade-off and define the efficient frontier. MVO operates without assumptions of Gaussian-distributed returns or quadratic investor utility functions (Kolm et al., 2014; Markowitz, 2010). Various paradigms rooted in classical and Bayesian statistical decision theory, as well as their causal extensions, have been applied to address different utility configurations. These encompass von Neumann and Morgenstern's theory, Savage's theory, rank-dependent utility theory, and prospect theory (Friedman and Savage, 1948; Heckerman and Shachter, 1995; Howard et al., 1972; Kahneman and Tversky, 1979; Lewis, 1981; Pearl, 1995; Ramsey, 1931; Savage, 1951; Schmidt, 2004; von Neumann et al., 1944). Beyond those foundational theories, the Black-Litterman model, a Bayesian approach for market-based shrinkage in portfolio optimization, incorporates investor views to refine market equilibrium implied expected returns and to enhance asset return covariance matrix estimation (Kolm et al., 2021). The risk parity approach distributes portfolio risk evenly across covered assets, aiming to withstand market downturns (Qian, 2005). The stochastic portfolio theory (SPT) employs Brownian motion to construct stochastic processes for asset prices, offering a descriptive instead of normative approach (Fernholz, 1999; Karatzas and Fernholz, 2009). Higher-moment portfolio theory recognizes the non-Gaussian properties of asset returns, aiming for improved returns and curtailed tail risks (Malevergne and Sornette, 2005). Robust portfolio theory acknowledges input estimate uncertainties, accounting for parameter uncertainty and model misspecification (Xidonas et al., 2020). In summary, a rich tapestry of compelling portfolio theories, each accompanied by corresponding objective functions, is documented in the literature, offering a diverse array of options for portfolio optimization.

The prevailing MVO framework integrates risk and alpha models. While risk models assess portfolio return variance, alpha models predict idiosyncratic expected returns. The advent of enhanced computing capabilities has

ushered in a new era for portfolio optimization, driven by generative models capable of simulating multivariate asset returns across a spectrum of market scenarios (Markowitz, 2014; Kolm et al., 2014). Generative model simulations drawn from model-implied predictions serve multiple crucial purposes, including model validation, goodness-of-fit assessment, software implementation evaluation, embedded research hypotheses refinement, and forecasts visualization (McElreath, 2020; Weinzierl, 2022). By harnessing generative model simulations for multivariate asset returns, we gain the capability to optimize performance metrics targeting moments, quantiles, and ordinals of the univariate portfolio return distribution.

Amidst the multitude of portfolio theories and the availability of generative models, decision-making becomes more diverse and fragmented. Individual investors often resort to a diverse set of mental models in their Swiss Army knife toolboxes (Munger and Kaufman, 2008). Discretionary portfolio managers working in silos allocate capital and influence institutional holdings. Research-oriented investment firms merge signals, blend portfolios, and make strategic shifts at a meta-level (De Prado, 2018). Market participants must navigate a complex landscape of risk-return trade-offs, time horizons, tax considerations, liquidity needs, and mandates. It might be advantageous for investors to opt for an eclectic portfolio, which can accommodate a range of portfolio theories and strategies, instead of adhering strictly to a single combination of proxy objective functions and generative models.

The literature has seen noteworthy efforts in addressing eclectic portfolio construction via portfolio blending through the lens of multi-armed bandit (MAB) problem-solving. Shen and Wang (2016) introduced an approach that leverages Thompson sampling for online portfolios, where they assign blending ratios  $\psi$  as probabilities for selecting from three basis portfolios, and adopt Bayesian decision rules to update the corresponding distribution functions. Assuming Bernoulli distribution for portfolio performances, the algorithm sequentially determines  $\psi$  to encapsulate a spectrum of investment criteria and market views. Remarkably, it demonstrates a distinct advantage over any individual basis portfolio across various market scenarios. In a similar vein, Fujishima and Nakagawa (2022) experiment with five basis portfolios within the MAB framework and assume Dirichlet distribution for portfolio performances to determine the blending ratio  $\psi$ . Their backtests show the potential benefits of blending in a cost-free transaction environment. Within

the MAB setting, the agent maintains a value model to evaluate the optimality among arms, and a policy model to decide which arm to pull either deterministically or stochastically. In defining the value model, it is imperative to establish a portfolio performance measure that not only accentuates decision quality but also remains comparable across a diverse array of portfolios and time steps. When crafting the policy model, achieving a balance in the concentration-diversification dilemma at the portfolio level becomes a necessity.

Cryptocurrencies have notably high correlations and their covariance matrices often possess elevated condition numbers. This attribute necessitates the application of advanced techniques in multivariate dependence modeling, asset returns generative modeling, and portfolio construction. This demand underscores the importance of evaluating and optimizing portfolio construction methodologies. Moreover, global cryptocurrency exchanges operate 24/7, facilitating the trading of homogeneous products with limited regulatory oversight. A multitude of participants have access to real-time price information, entering and exiting positions with the goal of profit maximization. These markets, with their unique characteristics, are still emerging and under-researched. This emerging terrain presents a fresh opportunity for advancing portfolio theory, which holds the potential to not only improve the management of cryptocurrency portfolios but also yield insights with broader applicability across financial markets.

In this paper, we embark on a comprehensive exploration of our portfolio construction framework, examining its foundation elements and efficacy evaluation. We first investigate and evaluate diverse pairings of generative models and objective functions. We then explore portfolio blending for constructing eclectic portfolios aligned with a wide array of investment strategies. We adapt the multi-armed bandit environment to the domain of portfolio blending. Within this MAB context, we propose similarity and optimality measures for value function estimates, and employ probability-matching (termed “blending”) or greedy algorithm (termed “switching”) for action selection policies. We show a framework for constructing superior eclectic portfolios through a thorough performance analysis of value model and policy model combinations. By conducting this exploration within the dynamic landscape of cryptocurrencies, we delve into an emerging area of finance that draws inspiration from multiple existing portfolio theories and practices. By doing

this, we aim to provide solutions and perspectives that have relevance not only in the cryptocurrency domain but also hold applicability across wider financial markets.

## 2. Constructing generative model-based portfolio: three essential components

The multi-period portfolio construction objective function can be formulated as follows:

$$\begin{aligned}
 & \max_{\mathbf{w}_{0,1}, \dots, \mathbf{w}_{0,t}, \dots, \mathbf{w}_{0,T}} \prod_{t=1}^T \left( 1 + r_{p,t}(\mathbf{w}_{0,t}, \mathbf{r}_t | \mathbf{w}_{1,t-1}, c) \right) \\
 & = \max_{\mathbf{w}_{0,1}, \dots, \mathbf{w}_{0,t}, \dots, \mathbf{w}_{0,T}} \prod_{t=1}^T \left( 1 + \mathbf{w}_{0,t} \mathbf{r}_t^T - c \|\mathbf{w}_{0,t} - \mathbf{w}_{1,t-1}\|_1 \right) \quad (1) \\
 & \quad s.t. \text{ constraints on } \mathbf{w}_{0,1}, \dots, \mathbf{w}_{0,t}, \dots, \mathbf{w}_{0,T}
 \end{aligned}$$

where  $\mathbf{r}_t \in \mathbb{R}^{1 \times D}$  is the row vector of asset returns from day  $t - 1$  to  $t \in \{1, 2, \dots, T\}$ ,  $D$  is the number of assets,  $T$  denotes the investment horizon,  $\mathbf{w}_{1,t-1} \in \mathbb{R}^{1 \times D}$  is the row vector of asset weights in the portfolio near the close of day  $t - 1$ , and  $c$  denotes the percentage transaction cost associated with weight changes. The scalar return of the portfolio  $r_{p,t}$  on day  $t$ , depends on  $\mathbf{r}_t$  and  $\mathbf{w}_{0,t}$ , as well as previous weights  $\mathbf{w}_{1,t-1}$  and transaction costs  $c$ . The decision vector  $\mathbf{w}_{0,t} \in \mathbb{R}^{1 \times D}$  is the row vector of asset weights of the portfolio at the close of day  $t - 1$ .

Note that  $\mathbf{r}_t$  remains unknown when  $\mathbf{w}_{0,t}$  is being determined. Therefore, all objective functions act as temporary approximations to eq. (1), relying either explicitly or implicitly on forecasts of multivariate asset returns  $\mathbf{r}_t$ . The cumulative product in eq. (1), which equally weights early and late portfolio gains, caters to rational, patient, and long-term investors. In practical applications, researchers often focus on one-period models due to the complexities associated with forecasting multivariate asset returns under real-world constraints (Lezmi et al., 2022).

In this paper, we optimize a one-period proxy objective function  $f(\cdot)$  (eq. (2)) targeting various performance metrics and risk-return appetites, subject to certain user-specific and time-specific constraints:

$$\begin{aligned} \max_{\mathbf{w}_0} f(\mathbf{w}_0 | R^{\mathbb{P}}, \mathbf{w}_1, c, v) \\ \text{s.t. } \|\mathbf{w}_0\|_1 = 1, w_{0,d} \in \left[-\frac{m}{D}, \frac{m}{D}\right], d \in \{1, 2, \dots, D\} \end{aligned} \tag{2}$$

where the decision vector  $\mathbf{w}_0 \in \mathbb{R}^{1 \times D}$  is the row vector of asset weights after rebalancing,  $\mathbf{w}_1 \in \mathbb{R}^{1 \times D}$  is the row vector of asset weights before rebalancing. The matrix  $R^{\mathbb{P}} \in \mathbb{R}^{N \times D}$  is filled with multivariate simulated asset returns drawn from generative models. Here  $N$  is the number of samples,  $c$  is the transaction cost,  $v$  is the scalar transaction-cost aversion coefficient (it is used to quantify a hurdle for trading), and  $m$  is the multiplier used in the weight box constraint.

The framework encompasses three essential components: generative models, proxy objective functions, and optimization constraints. Optimization constraints are indispensable but case-specific in real-world applications. In an order that is easier to comprehend, we successively discuss constraints, proxy objective functions, and generative models.

### 2.1. Constraints

Constraints play a pivotal role in enhancing out-of-sample performance by mitigating volatility, preventing over-concentration, and reducing downside risk. Constraints can originate from a variety of sources: regulatory policies, client guidelines, discretionary exposure limits, compliance requirements, and considerations related to market volume, reflexivity, and liquidity (Kolm et al., 2014; Soros, 2013). Selecting and formulating constraints often involves a degree of subjectivity, making it more an eclectic art than a science, as it necessitates judgment and consideration of multiple factors. Markowitz emphasized that if the one-sum (Roy, 1952) is the sole constraint on portfolio choice, the resulting negative weights are far from an accurate representation of real-world positions (Markowitz, 2010).

In this study, without loss of generality, we set the following constraints when solving eq. (2):

$$\begin{aligned} \|\mathbf{w}_0\|_1 &= 1 \\ w_{0,d} &\in \left[-\frac{m}{D}, \frac{m}{D}\right] \end{aligned}$$

where  $D$  is the number of assets covered in each portfolio, and we typically use  $m = 5$  for the weight constraint. This  $L1$ -norm equality constraint is conservative and allows for both equally long weights and equally short weights. In practice, investors can utilize  $\|\mathbf{w}_0\|_1 = l$ ,  $l > 0$  to meet permitted leverages levels.

## 2.2. Proxy objective functions

### 2.2.1. Kelly portfolio

According to the standard Kelly criterion (Kelly Jr., 1956; Thorp, 1975), when allocating  $1 - w$  to a risk-free zero return asset and  $w \in (0, 1)$  to a risk-bearing asset which has a probability  $p \in (0, 1)$  to gain  $b$  and  $(1 - p)$  to lose  $a$ , the objective function for determining  $w$  (assuming the number of periods  $N \rightarrow \infty$  and no transaction costs) is:

$$\begin{aligned} & \max_w Np \log(1 + wb) + N(1 - p) \log(1 - wa) \\ & \text{s.t. } w \in (0, 1) \end{aligned}$$

Let  $\mathbf{w}_0 = [w, 1 - w]$  be a row vector for weights,  $\mathbf{p} = [p, 1 - p]^T$  be a column vector for probability mass function, and  $R = \begin{pmatrix} b & 0 \\ -a & 0 \end{pmatrix}$  be a matrix of asset return scenarios. To generalize Kelly's objective function for multiple assets, we use the Hadamard (element-wise) product notation  $\odot$ :

$$\begin{aligned} & \max \mathbf{p}^T \log(1 + R\mathbf{w}_0^T) \\ & = \max \sum \sum \mathbf{p} \odot \log(1 + R \odot \mathbf{w}_0) \\ & \approx \max \sum \sum \log(1 + \mathbf{p} \odot R \odot \mathbf{w}_0) \end{aligned} \quad (3)$$

The approximation in eq. (3) holds when the absolute values of elements in  $R \odot \mathbf{w}$  are much smaller than 1, which is typically the case in well-diversified portfolios over a single period. Let  $R^{\mathbb{P}} \in \mathbb{R}^{N \times 2}$  be a tall matrix with  $p$  proportion of rows as  $[b, 0]$  and the rest as  $[-a, 0]$ . After absorbing the effect of  $\mathbf{p}$  into  $R^{\mathbb{P}}$ , we have:

$$\begin{aligned} & \max \sum \sum \log(1 + R^{\mathbb{P}} \odot \mathbf{w}_0) \\ & \approx \max \sum \sum \left( R^{\mathbb{P}} \odot \mathbf{w}_0 - \frac{(R^{\mathbb{P}} \odot \mathbf{w}_0)^2}{2} + \frac{(R^{\mathbb{P}} \odot \mathbf{w}_0)^3}{3} - \frac{(R^{\mathbb{P}} \odot \mathbf{w}_0)^4}{4} \right) \end{aligned}$$

This proxy objective function can accommodate more assets with longer  $\mathbf{w}_0$  and a wider  $R^{\mathbb{P}}$ . The Kelly portfolio employs portfolio log return  $\log(1 + r_p)$  instead of portfolio simple return  $r_p$  as its objective function, leading to diminishing marginal utility and tail loss aversion. Unlike traditional portfolio construction, where risk-free assets with zero variances and covariances are considered separately as a leveraging concern, the Kelly portfolio can be seamlessly integrated into the asset portfolio construction process.

In this paper, we use the following Kelly portfolio proxy objective function:

$$\max \sum \log(1 + \mathbf{r}_p)$$

where  $\mathbf{r}_p(\mathbf{w}_0|R^{\mathbb{P}}, \mathbf{w}_1, c, v) = R^{\mathbb{P}} \mathbf{w}_0^T - c v \|\mathbf{w}_0 - \mathbf{w}_1\|_1$ ,  $\mathbf{r}_p \in \mathbb{R}^{N \times 1}$  is the column vector of possible portfolio returns  $r_p$ ,  $c$  denotes the constant transaction, and  $v$  is a transaction cost aversion coefficient, which is used to control portfolio turnover.

This objective function shares a close relationship with eq. (1). Its construction relies on complete distribution information, going beyond first or second-moment statistics. Its primary focus is on maximizing the portfolio’s long-term growth rate with no explicit consideration of investor risk aversion. Consequently, this approach can lead to overly aggressive bets. In practice, the objective function can be adapted by truncating at finite moments and adjusting the coefficients associated with  $R^{\mathbb{P}} \odot \mathbf{w}_0$  series to accommodate various risk-return trade-off considerations. Moreover, by maximizing the geometric mean of portfolio returns instead of the arithmetic mean, the Kelly portfolio mitigates the “volatility drag” associated with long-term portfolio returns (Lo and Foerster, 2021). Implementing the Kelly portfolio may encounter numerical problems when  $1 + \mathbf{r}_p(\mathbf{w}_0|R^{\mathbb{P}}, \mathbf{w}_1, c, v) \leq 0$ . This issue can be circumvented by confining the search for optimal  $\mathbf{w}_0$  in the subspace where  $1 + \mathbf{r}_p(\mathbf{w}_0|R^{\mathbb{P}}, \mathbf{w}_1, c) > 0$ .

### 2.2.2. Finite-moments portfolio

The Markowitz-Roy portfolio is formulated using the following general objective function:



$$\begin{aligned} & \max \lambda_1 \mathbb{E}[r_p] - \lambda_2 \mathbb{V}[r_p] \\ & = \max \lambda_1 (\mathbf{1} R^{\mathbb{P}} \mathbf{w}_0^T) - \lambda_2 (\mathbf{1} (R^{\mathbb{P}} \mathbf{w}_0^T)^2 - (\mathbf{1} R^{\mathbb{P}} \mathbf{w}_0^T)^2) \end{aligned}$$

where  $\mathbf{1} \in \mathbb{R}^{1 \times N}$  are row vectors. Several finite-moments-based metrics in this form are proposed in the literature. Given the first and second moments in MVO, the maximum entropy distribution is the Gaussian distribution, which allows for exact solutions or accelerated numerical solutions in finite-moment cases.

In this study, we explore a range of finite-moments-based proxy objective functions, targeting portfolio variance (4), expectation (5), downside frequency (6), downside variance (7) (Roy, 1952), Sharpe ratio (8) (Sharpe, 1966), Sortino ratio (9) (Sortino and Price, 1994), and Bernado-Ledoit ratio (10) (Bernardo and Ledoit, 2000):

$$\min \mathbb{E} [(r_p - \mathbb{E}[r_p])^2] \tag{4}$$

$$\min -\mathbb{E}[r_p] \tag{5}$$

$$\min \mathbb{E}[\mathbb{I}(r_p < 0)] \tag{6}$$

$$\min \mathbb{E}[r_p^2 | r_p < 0] \tag{7}$$

$$\min -\log(100 + \mathbb{E}[r_p]/\sigma_1) \tag{8}$$

$$\min -\log(100 + \mathbb{E}[r_p]/\sigma_2) \tag{9}$$

$$\min \log(\mathbb{E}[|r_p|] + \mathbb{E}[|r_p| | r_p < 0]) - \log(\mathbb{E}[|r_p|]) \tag{10}$$

where  $\mathbf{r}_p = R^{\mathbb{P}} \mathbf{w}_0^T - c v \|\mathbf{w}_0 - \mathbf{w}_1\|_1$ ,  $\sigma_1^2 = \mathbb{E}[(r_p - \mathbb{E}[r_p])^2]$  and  $\sigma_2^2 = \mathbb{E}[r_p^2 | r_p < 0]$ .

### 2.2.3. Quantile portfolio

We also investigate portfolio proxy objective functions targeting Value-at-Risk (VaR) (Longerstaey and Spencer, 1996) and Expected Shortfall (ES) (Rockafellar et al., 2000) for constructing quantile portfolios:

$$\begin{aligned} & \max \int_0^1 F_p^{-1}(u) \delta(u - \alpha) du \\ & \max \int_0^1 F_p^{-1}(u) \frac{\mathbb{I}(u \in (0, \alpha))}{\alpha} du \end{aligned}$$

where  $F_p^{-1}(\cdot)$  is the percent point function (PPF) of the portfolio return  $r_p$ ,  $\delta(\cdot)$  is Dirac's delta function, and  $\alpha \in \{0.05, 0.1, 0.5\}$ .

They are spectral risk measures (Acerbi, 2002) that can address the tail part of the  $r_p$  distribution. Tail profit/loss events, often challenging to quantify, exert more influence on investment decisions than average profit and loss. As widely accepted tail risk measures, ES is a coherent risk measure but VaR is not.

#### 2.2.4. Parity portfolio

Parity portfolios are constructed using heuristic proxy objective functions that target long weight parity (“Talmud”) (11), short weight parity (12), and variance parity (13) (Qian, 2011):

$$\begin{aligned} & \max \cos(\mathbf{w}_0, \mathbf{1}) \\ & = \max \frac{\mathbf{w}_0}{\|\mathbf{w}_0\|_2} \cdot \mathbf{1} \end{aligned} \tag{11}$$

$$\begin{aligned} & \max \cos(\mathbf{w}_0, -\mathbf{1}) \\ & = \max -\frac{\mathbf{w}_0}{\|\mathbf{w}_0\|_2} \cdot \mathbf{1} \end{aligned} \tag{12}$$

$$\begin{aligned} & \max \cos(\mathbf{w}_0 \odot \sigma^2, \mathbf{1}) \\ & = \max \frac{\mathbf{w}_0 \odot \sigma^2}{\|\mathbf{w}_0 \odot \sigma^2\|_2} \cdot \mathbf{1} \end{aligned} \tag{13}$$

where  $\sigma \in \mathbb{R}^{1 \times D}$  is a row vector filled with the standard deviation of assets returns  $\sigma_d = \sqrt{\mathbb{V}(r_d w_{0,d} - c v \|w_{0,d} - w_{1,d}\|_1)}$ , and  $r_d$  denotes the return of asset  $d$ . Both  $\sigma \in \mathbb{R}^{1 \times D}$  and  $\mathbf{1} \in \mathbb{R}^{1 \times D}$  have the same shape as  $\mathbf{w}_0 \in \mathbb{R}^{1 \times D}$ .

#### 2.3. Forecasting from generative models

Forecasting is explicitly or implicitly embedded in any portfolio construction scheme. Accurate multivariate asset return dependence modeling is important for diversification in investment portfolios. The generative model approach uses a rolling window of observed historical returns to learn the coherent structure of asset performances over time, and to generate future asset returns. Multivariate elliptical distributions, including multivariate Gaussian and Student's t, are widely accepted in academia and industry for their efficiency and well-understood properties. Notably, the dynamic conditional

correlation (DCC)-generalized autoregressive conditional heteroskedasticity (GARCH) model addresses both individual asset volatility clustering and time-varying cross-asset correlations (Orskaug, 2009). On another front, copula models are designed to disentangle marginal univariate distributions from multivariate dependence patterns (Joe, 2014). Vine copula models, in particular, have emerged as a versatile tool for constructing multivariate copulae using bivariate building blocks and conditionalizing, allowing for flexible modeling of multivariate asymmetric tail dependencies (Czado et al., 2022).

The univariate GARCH (1, 1) model is defined as:

$$\begin{aligned} r_t &= \mu_t + a_t \\ a_t &= h_t^{1/2} z_t \\ h_t &= \alpha_0 + \alpha_1 a_{t-1}^2 + \beta_1 h_{t-1} \end{aligned}$$

where  $r_t$  is the return,  $a_t$  is the mean-corrected return,  $z_t$  is the standardized error independent and identically distributed (i.i.d.) in  $N(0, 1)$ ;  $\alpha_0, \alpha_1, \beta_1$  are parameters. The conditional variance  $h_t$  is determined based on historical returns. Forecasts of  $r_t$  can be generated from samples of  $z_t$  (Bollerslev, 1986).

The multivariate DCC(1,1)-GARCH(1,1) model takes the following form (Engle, 2002):

$$\begin{aligned} \mathbf{r}_t &= \boldsymbol{\mu}_t + \mathbf{a}_t \\ \mathbf{a}_t &= \mathbf{z}_t \mathbf{H}_t^{1/2} \\ \mathbf{H}_t &= \mathbf{G}_t \mathbf{R}_t \mathbf{G}_t \\ \mathbf{G}_t &= \text{diag}[\sqrt{h_{1,t}}, \dots, \sqrt{h_{d,t}}, \dots, \sqrt{h_{D,t}}] \\ h_{i,t} &= \alpha_{i,0} + \alpha_{i,1} a_{i,t-1}^2 + \beta_{i,1} h_{i,t-1} \\ \mathbf{R}_t &= \mathbf{Q}_t^* \mathbf{Q}_t^* \mathbf{Q}_t^* \mathbf{Q}_t^* \\ \mathbf{Q}_t^* &= \text{diag}[\sqrt{q_{11,t}}, \dots, \sqrt{q_{dd,t}}, \dots, \sqrt{q_{DD,t}}] \\ \mathbf{Q}_t &= (1 - a - b) \bar{\mathbf{Q}} + a \boldsymbol{\epsilon}_{t-1}^T \boldsymbol{\epsilon}_{t-1} + b \mathbf{Q}_{t-1}, \quad a \geq 0, b \geq 0, a + b < 1 \\ \boldsymbol{\epsilon}_t &= \mathbf{a}_t \mathbf{G}_t^{-1} \sim N(\mathbf{0}, \mathbf{R}_t) \\ \bar{\mathbf{Q}} &= \text{Cov}[\boldsymbol{\epsilon}_t^T \boldsymbol{\epsilon}_t] = \mathbb{E}[\boldsymbol{\epsilon}_t^T \boldsymbol{\epsilon}_t], \end{aligned}$$

where  $\mathbf{r}_t \in \mathbb{R}^{1 \times D}$  is a row vector for returns of  $D$  assets,  $\mathbf{a}_t \in \mathbb{R}^{1 \times D}$  is a row vector of mean-corrected returns,  $\mathbf{H}_t \in \mathbb{R}^{D \times D}$  is the positive definite (p.d.) conditional covariance of  $\mathbf{a}_t$ ,  $\mathbf{z}_t \in \mathbb{R}^{1 \times D}$  is a row vector of i.i.d. errors distributed in multivariate Gaussian or Student's t.  $\mathbf{G}_t \in \mathbb{R}^{D \times D}$  as a p.d. diagonal matrix has standard deviations from univariate GARCH(1, 1) models.  $\mathbf{R}_t \in \mathbb{R}^{D \times D}$  is the p.d. conditional correlation matrix of the standardized disturbances row vector  $\epsilon_t \in \mathbb{R}^{1 \times D}$ .  $\bar{\mathbf{Q}} \in \mathbb{R}^{D \times D}$  is the p.d. unconditional covariance matrix of the standardized errors (which can be estimated as time series averages), and  $\mathbf{Q}_t^* \in \mathbb{R}^{D \times D}$  is a p.d. diagonal matrix with entries from the square root of the diagonal elements of  $\mathbf{Q}_t \in \mathbb{R}^{D \times D}$ .  $\mathbf{Q}_t^*$  is designed to rescale elements in  $\mathbf{Q}_t$ . Forecasts of  $\mathbf{r}_t$  can be generated from samples of  $\mathbf{z}_t$ .

Dependency modeling using copulas is based on Sklar's theorem,

$$\begin{aligned} F(x_1, \dots, x_D) &= C(F_1(x_1), \dots, F_D(x_D)) \\ F(F_1^{-1}(u_1), \dots, F_D^{-1}(u_D)) &= C(u_1, \dots, u_D) \end{aligned}$$

where  $F$  is the multivariate cumulative distribution function (CDF) of  $X_1, \dots, X_D$ ,  $C$  is the associated copula,  $F_d, d \in \{1, \dots, D\}$  are marginal CDFs, and  $F_d^{-1}$  are marginal PPF or the inverse of marginal CDF (Joe, 2014).

The multivariate Gaussian copula has the form,

$$C(\mathbf{u}; \mathbf{R}) = \Phi_D(\Phi^{-1}(u_1), \dots, \Phi^{-1}(u_D); \mathbf{R})$$

where  $\Phi_D$  and  $\Phi$  are the multivariate and univariate Gaussian CDF, and  $\mathbf{R} \in \mathbb{R}^{D \times D}$  is the p.d. correlation matrix. Simulations of this copula could be done by taking standard Gaussian CDF on samples from multivariate Gaussian distribution whose covariance matrix is  $\mathbf{R}$ . Forecasts of asset returns can then be generated by taking marginal PPF (Paolella and Polak, 2018).

The multivariate Student's t copula has the form,

$$C(\mathbf{u}; \mathbf{R}, \nu) = T_{D, \nu}(T_{1, \nu}^{-1}(u_1), \dots, T_{1, \nu}^{-1}(u_D); \mathbf{R})$$

where  $T_{D,\nu}$  and  $T_{1,\nu}$  are the multivariate and univariate Student’s t CDFs with the same degree of freedom  $\nu$ , and  $\mathbf{R} \in \mathbb{R}^{D \times D}$  is the p.d. correlation matrix. A similar procedure can be used to generate asset return forecasts from this copula.

The regular vine copulae are constructed recursively. For every pair of bivariate copulae data, we fit pair copula from elliptical or Archimedean families by maximum likelihood estimation (MLE) and select the one with minimal Akaike information criterion (AIC) (Akaike, 1998). The regular vine copula structure is constructed by picking the maximum spanning tree, which maximizes the sum of absolute values of Kendall’s  $\tau$  among pairwise variables while adhering to proximity conditions (Dißmann et al., 2013). Simulations of this copula could be done by performing inverse Rosenblatt transform (Rosenblatt, 1952) on i.i.d. multivariate uniform samples (Czado, 2019). Forecasts of asset returns can then be generated by taking marginal PPF.

In this study, we cover a diverse set of generative models for asset returns forecasting. The asset returns in historical windows, available at every rebalancing step, are used as inputs to fit generative models. We fit multivariate Gaussian and Student’s t distributions, multivariate Gaussian and Student’s t copulae, and regular-vine copulae using combinations of elliptical family copulae and Archimedean family copulae. We build DCC(1,1)-GARCH(1,1) models using Gaussian and Student’s t-distributed errors. To address temporal serial correlation before modeling dependency across assets, we also include models where residuals from univariate GARCH(1,1) models are fed to Gaussian, Student’s t, and Vine copulae. Both parametric and non-parametric (empirical) univariate marginal CDF and PPF are used to process returns into copula data. We consider a range of candidate parametric marginal CDFs including Gaussian, Student’s t, non-central Student’s t, Johnson’s SU, Tukey-lambda, Laplace, and asymmetric Laplace distributions. Fitted marginals are selected to minimize AIC. All parametric models are fitted by MLE using historical observed data.

#### 2.4. Backtest

To backtest generative model-based portfolios, we retrieved price time series from Binance, spanning from 2018-06-10 to 2023-06-04, covering 12 currencies priced in USDT including ADA, BNB, BTC, EOS, ETH, IOTA, LTC, NEO, ONT, QTUM, XLM, and XRP. As depicted in fig. 1, asset returns

have notable high correlations. Rebalancing occurs every two days, targeting diverse combinations of generative dependence model forecasts and proxy objective functions. To fit the generative model, we employ a rolling window length of 91 steps or 182 days. The transaction cost  $c$  is set as 50 bps, together with the number of assets  $D = 12$  and the constraint boundary multiplier  $m = 5$ . To ensure robustness and assess performance consistency, we conduct multiple independent simulations using different random seeds. In total, we have 6525 simulation paths, each comprising 820 steps.

For performance attribution, we fit the least absolute shrinkage and selection operator (LASSO) model (14) and analyze portfolio performance at each step (Efron et al., 2004; Pedregosa et al., 2011). We use the portfolio simple return  $r_p$  (15) and the logit of cosine similarity between  $\mathbf{w}_{0,t}$  and  $\mathbf{r}_t$  (16) as the performance measure  $y$ . In eq. (16), the cosine similarity is used to quantify decision quality, and the logit transform extends its value from  $(0, 1)$  to the entire real line. The whole logit-cosine performance measure is designed to be a consistent ex-post metric, enabling comparisons of simulation outcomes at different steps from different generative model / objective function setups. The LASSO model, known for its capacity to produce sparse yet robust coefficients, is employed primarily for its interpretable coefficient ranking.

$$\min \frac{1}{2 n_{\text{samples}}} \|\mathbf{y} - \mathbf{X}\hat{\beta}\|_2^2 + \lambda \|\hat{\beta}\|_1 \quad (14)$$

$$y = r_p \quad (15)$$

$$y = \text{logit} \left( \frac{1 + \cos(\mathbf{w}_{0,t}, \mathbf{r}_t)}{2} \right) \quad (16)$$

The design matrix  $\mathbf{X} \in \mathbb{R}^{5350500 \times 597}$  is filled with binary values (0 or 1) encoding the presence of foundation elements for portfolio construction: the intercept, various generative models, objective functions, the transaction cost aversion coefficient  $v$ , and specific combinations of them (as interaction terms indicating the simultaneous presence of the underlying elements). While  $\mathbf{X}$  possesses 597 columns, each row contains only seven instances of the value 1. The performance measures, represented as the column vector  $\mathbf{y} \in \mathbb{R}^{5350500 \times 1}$  encompass data from all steps in all simulation paths. As the scalar regularization strength hyper-parameter  $\lambda$  increases, sparser  $\hat{\beta} \in \mathbb{R}^{597 \times 1}$  estimates are obtained. The regularization process results in the shrinkage of coeffi-

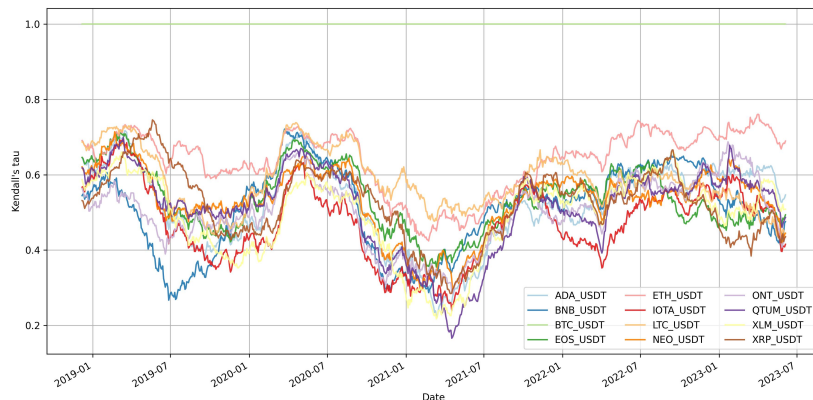


Figure 1: Kendall's  $\tau$  between BTC and studied cryptocurrencies, using a 182-day rolling window of 2-day simple returns as priced in USDT on Binance.

cients for unimportant covariates, effectively reducing them to 0. Any remaining influence from these unimportant covariates is typically aggregated within the intercept term. The optimal  $\lambda^*$  is selected based on 7-fold cross-validation (CV) that minimizes mean squared error (MSE). For illustration, we visualize the MSE paths in each fold during CV for  $r_p$  in fig. 2a and coefficient paths during the final fit using all observations for  $r_p$  in fig. 2b.

The cumulative sum of logit-cosine performance measure is visualized in fig. 3. The symmetry of the logit-cosine performance measure is shown in fig. 3b where lines representing the long-weight parity portfolio and the short-weight parity portfolio are mirrored around the horizontal axis. We present the non-zero coefficients obtained at the optimal  $\lambda^*$  in LASSO for the  $r_p$  in table 1 and for the logit-cosine performance measure in table 2.

In general, during the periods we considered, the cryptocurrency market (priced in USDT) exhibited an upward trend as indicated by the positive intercept term in both tables. The choice of the proxy objective function is shown to have a greater impact as evidenced by the larger magnitude of their coefficients in both tables. Among the generative models, only the vine copula yields positive coefficients in both tables, emphasizing its superiority in multivariate dependence modeling. It's worth noting that interaction terms corresponding to the presence of specific combinations of the generative model and objective function have shrunk to 0. This suggests that it is rea-

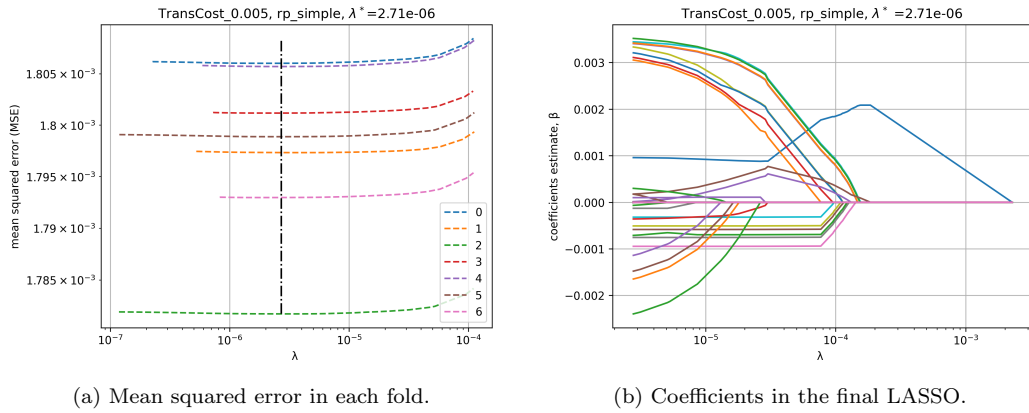


Figure 2: Cross-validated LASSO paths for portfolio return  $r_p$  attribution. The optimal regularization strength hyperparameter  $\lambda^*$  is the average of  $\lambda$  where mean squared errors are minimized in each fold.

sonable to divide the portfolio construction task into asset return forecasting and optimizations. The Sharpe ratio portfolios, as classical finite-moments portfolios, outperformed Kelly’s portfolios, quantile portfolios, and parity portfolios.

To illustrate the best combination suggested by the LASSO results, we chart the cumulative returns of portfolios using parametric marginal distribution and vine copulas based on Archimedean bivariate copula as the generative model paired with Sharpe ratio as the objective function in fig. 4a. Their averaged asset weights are depicted in fig. 4b. Notably, all simulated paths generated using this combination outperformed the benchmark, which adheres to the long-weight parity objective function but with no transaction costs included in the portfolio return. A moderate transaction cost aversion coefficient  $v$  around 2 to 3 is favorable, but too high a hurdle for trading could limit terminal profits. These portfolios often contain a strong long position in BNB, ETH, ADA, and BTC, and even reach the upper weight limit  $m/D$  for BNB occasionally.

### 3. Constructing eclectic portfolios: three essential components

In this session, we expand our exploration beyond the confines of a single combination of proxy objective functions and generative model forecasts. We delve into the realm of portfolio blending, embracing diverse portfolio



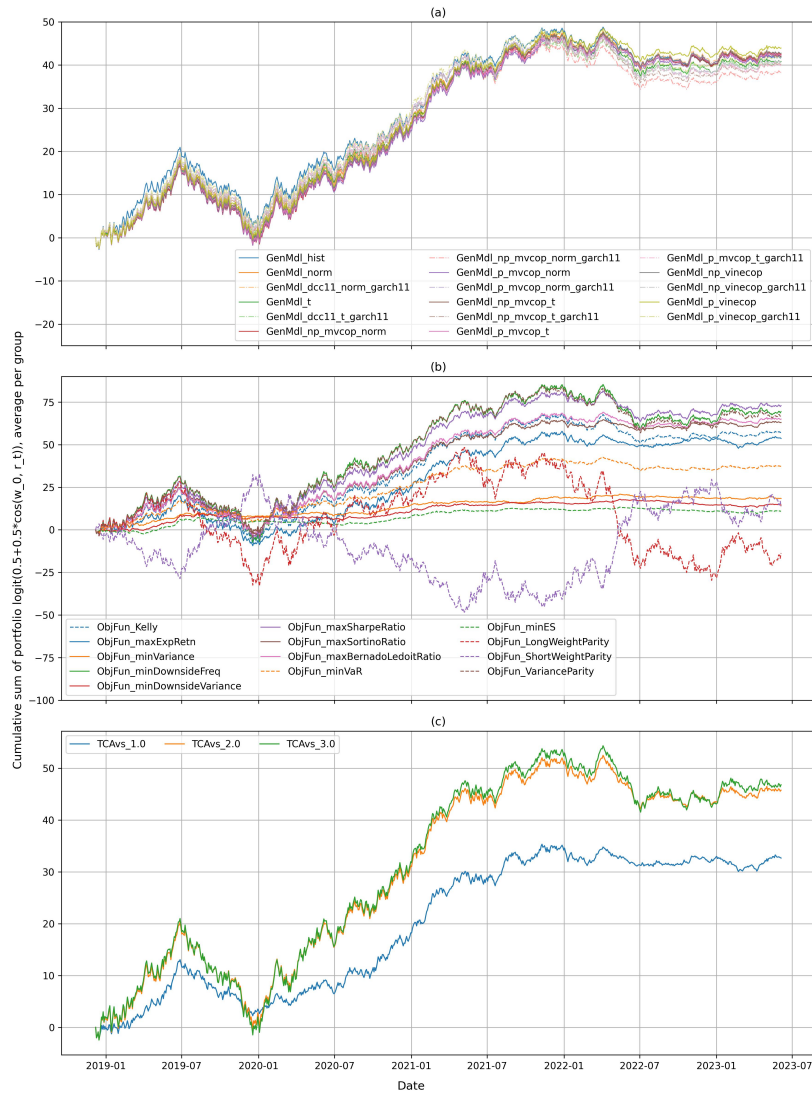


Figure 3: Cumulative sum of logit-cosine performance measure, averaged for portfolios grouped by (a) asset returns generative models, (b) proxy objective functions and (c) transaction cost aversion coefficients.

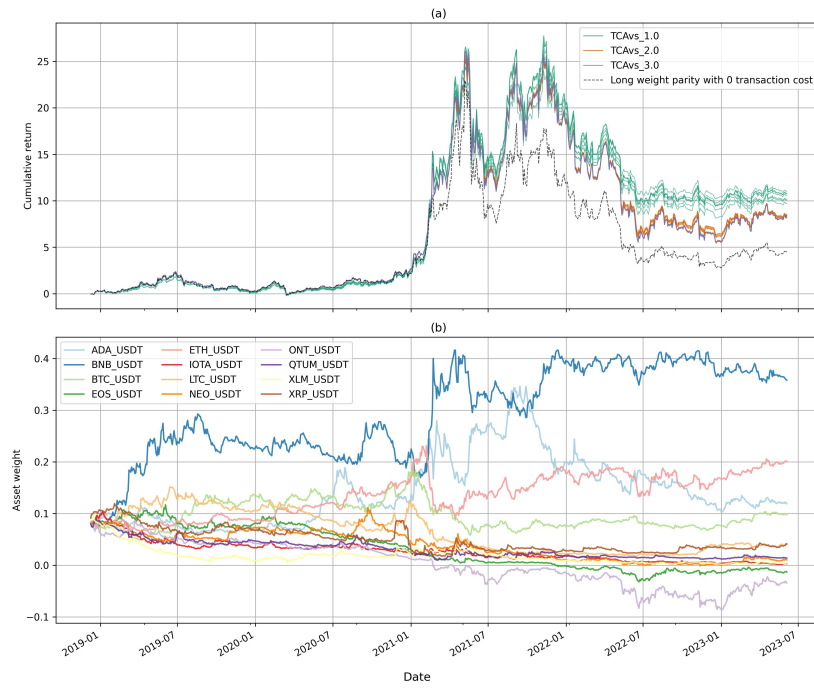


Figure 4: Visualization of portfolios using vine copula with parametric univariate marginal distributions and Archimedean bivariate copulae as asset returns forecasting generative models along with Sharpe ratio maximization as proxy objective functions, in (a) cumulative simple returns and (b) averaged asset weights.

Table 1: Non-zero coefficients in LASSO for portfolio simple return, corresponding to combinations of proxy objective functions, generative models, and transaction cost aversion coefficients.

coefficient	value
ObjFun maxSharpeRatio	0.003516
ObjFun VarianceParity	0.003443
ObjFun minVaR 0.5	0.003415
ObjFun minDownsideFreq	0.003403
ObjFun Kelly	0.003332
ObjFun maxBernadoLedoitRatio	0.003207
ObjFun maxSortinoRatio	0.003107
ObjFun maxExpRetn	0.003051
intercept	0.000958
ObjFun VarianceParity : TCavs 1.0	0.000297
TCavs 3.0	0.000175
ObjFun minVariance : TCavs 1.0	0.000173
ObjFun maxExpRetn : TCavs 3.0	0.000098
TCavs 2.0	0.000013
GenMdl p vinecop archimedean	0.000002
GenMdl np vinecop garch11 elliptical	-0.000010
GenMdl dcc11 t garch11	-0.000067
ObjFun minVariance : TCavs 3.0	-0.000131
ObjFun minVaR 0.05	-0.000321
TCavs 1.0	-0.000360
ObjFun minES 0.5	-0.000509
ObjFun minDownsideVariance	-0.000585
ObjFun minVariance	-0.000712
ObjFun minES 0.1	-0.000757
ObjFun minES 0.05	-0.000947
ObjFun maxBernadoLedoitRatio : TCavs 1.0	-0.001141
ObjFun Kelly : TCavs 1.0	-0.001479
ObjFun maxSortinoRatio : TCavs 1.0	-0.001648
ObjFun maxExpRetn : TCavs 1.0	-0.002397

theories and strategies. Our approach, as outlined in section 2, involves an extension of the MAB framework.

In the classical MAB Markov decision process, a decision-maker seeks to maximize rewards obtained from a limited number of lever pulls on slot machines. In other words, the agent interacts with a one-state environment and searches for the best action (Sutton and Barto, 2018; Thompson, 1933). In our context, the agent’s action space corresponds to the set of arms representing different portfolio choices, and the environment’s rewards associated with each arm are determined by the performance of the corresponding portfolio. The agent holds both a value model to evaluate the relative optimality among arms, and also a policy model to decide which arm to pull.

Table 2: Non-zero coefficients in LASSO for the logit-cosine performance measure, corresponding to combinations of proxy objective functions, generative models, and transaction cost aversion coefficients.

coefficient	value
ObjFun maxSharpeRatio	0.058424
ObjFun maxBernadoLedoitRatio	0.054276
ObjFun minDownsideFreq	0.054091
ObjFun minVaR 0.5	0.051835
ObjFun maxExpRetn : TCavs 2.0	0.050512
ObjFun Kelly	0.049198
ObjFun maxExpRetn : TCavs 3.0	0.047490
ObjFun VarianceParity	0.047314
ObjFun maxSortinoRatio : TCavs 2.0	0.034248
intercept	0.031102
ObjFun maxSortinoRatio : TCavs 3.0	0.028144
ObjFun maxSortinoRatio	0.025601
ObjFun VarianceParity : TCavs 1.0	0.013741
ObjFun minVaR 0.5 : TCavs 1.0	0.007737
TCavs 3.0	0.002453
GenMdl p vinecop archimedean	0.002403
ObjFun maxBernadoLedoitRatio : TCavs 2.0	0.002340
ObjFun maxExpRetn	0.002289
ObjFun Kelly : TCavs 2.0	0.001262
GenMdl p vinecop allfam	0.000581
ObjFun minDownsideFreq : TCavs 1.0	0.000114
GenMdl dcc11 t garch11	-0.000200
GenMdl p mvcop t garch11	-0.000259
GenMdl np vinecop garch11 allfam	-0.000993
ObjFun minDownsideVariance : TCavs 1.0	-0.001419
GenMdl np mvcop norm garch11	-0.002232
ObjFun minVariance	-0.004122
ObjFun minVaR 0.05	-0.004588
ObjFun minVariance : TCavs 3.0	-0.004930
ObjFun minES 0.5	-0.006759
TCavs 1.0	-0.007696
ObjFun minDownsideVariance	-0.010017
ObjFun minES 0.1	-0.016901
ObjFun maxBernadoLedoitRatio : TCavs 1.0	-0.018773
ObjFun minES 0.05	-0.020972
ObjFun Kelly : TCavs 1.0	-0.030433

Eclectic portfolios are constructed by allocating blending ratios  $\psi \in \mathbb{R}^{1 \times P}$  to portfolios of different investment styles. At each step, the agent updates the fractional blending ratio  $\psi_p$  for each portfolio  $p$ , based on their historical performances up to that point. In other words, we work towards eq. (1) by blending optimal weights solved from different one-period eq. (2) in a long-only manner ( $\|\psi\|_1 = 1$ ,  $\psi_p > 0$ ). The temporal coherence exhibited in the market dynamics and portfolio performances allows such reinforcement

learning to explore better portfolio blending.

Three components are essential: similarity, optimality, and blending ratio. Similarity, denoted as  $s(\cdot)$ , defines comparable portfolio performance metrics. Optimality quantifies arm preferences among peers using activation functions  $\pi(\cdot)$ . Blending ratios  $\psi(\cdot)$  determine the allocation strategy. In essence,  $s(\cdot)$  and  $\pi(\cdot)$  constitute the value model, while  $\psi(\cdot)$  encodes the policy model.

Practical principles are embedded in this reinforcement learning task. Better-performing arms should have higher  $s(\cdot)$  and  $\pi(\cdot)$  in value models. Since the market is adaptive (Lo, 2017), recent performances should carry more weight in policy models.

### 3.1. Similarity

The initial step involves reviewing recent portfolio weights to compute comparable performance statistics across various portfolios. This measure should highlight decision quality, be comparable at different time steps, be positively correlated to portfolio returns, and not be specific to  $\mathbf{w}_{1,t-1,p}$ ,  $c$ , and  $v$ .

We calculate the ex-post similarity row vector  $\mathbf{s}_t \in \mathbb{R}^{1 \times P}$  by assessing how closely the realized asset returns  $\mathbf{r}_t$  align with the solutions  $\mathbf{w}_{0,t,p}$  obtained from eq. (2), where  $t$  denotes the time step and  $P$  represents the number of arms or portfolios.

The cosine similarity of portfolio  $p \in \{1, 2, \dots, P\}$  is the cosine of the angle between  $\mathbf{w}_{0,t,p} \in \mathbb{R}^{1 \times D}$  and  $\mathbf{r}_t \in \mathbb{R}^{1 \times D}$ :

$$s_{\text{cos},t,p} = \frac{\mathbf{w}_{0,t,p} \cdot \mathbf{r}_t}{\|\mathbf{w}_{0,t,p}\|_2 \|\mathbf{r}_t\|_2}$$

The Z-score similarity is defined as:

$$s_{Z,t,p} = 2 \Phi(\mathbf{w}_{0,t,p} \cdot \mathbf{r}_t) - 1$$

where  $\Phi(\cdot)$  is the CDF of standard Gaussian distribution.

Other similarities based on the vector norms of  $\mathbf{d}_{t,p} = \frac{\mathbf{w}_{0,t,p}}{\|\mathbf{w}_{0,t,p}\|_1} - \frac{\mathbf{r}_t}{\|\mathbf{r}_t\|_1}$  (which is the distance between two points on an  $L1$  unit sphere) are also used:

$$\begin{aligned}
s_{L1,t,p} &= 1 - \|\mathbf{d}_{t,p}\|_1 \\
s_{L2,t,p} &= 1 - \|\mathbf{d}_{t,p}\|_2 \\
s_{L\infty,t,p} &= 1 - \|\mathbf{d}_{t,p}\|_\infty
\end{aligned}$$

All of the above measures use re-scaled returns to focus on the decision quality of an arm. These measures are bounded inside  $[-1, 1]$  and are strongly correlated with portfolio returns.

### 3.2. Optimality

The second step is to assess the optimality of each portfolio  $p$  among peers  $\pi_{t,p}$ , by applying activation functions to similarities.

The naive greedy activation function is the maxout eq. (17), which compares the similarities of different portfolios at the same time step  $t$ , then assigns a grade of 1 to those with the highest  $s(\cdot)$  and 0 to the rest. We rescale grades  $\mathbf{g}_t \in \mathbb{R}^{1 \times P}$  of portfolios  $p$  by sum to get  $\pi_{t,p}$  if there are ties.

$$\begin{aligned}
g_{t,p} &= \mathbb{I}\{p = \arg \max_q (s_{t,q})\} \\
\pi_{t,p} &= \frac{g_{t,p}}{\|\mathbf{g}_t\|_1}
\end{aligned} \tag{17}$$

The optimality scores are organized in a matrix, where the column indexes a portfolio  $p$  and the row indexes a previous step  $t$ . If there are multiple strategies to evaluate, the matrix  $\pi_{t,p}$  filled with the maxout activation function will be wide and sparse. This study also explores non-greedy activation functions including softmax (18), logistic (19), tanh (20), leaky-relu (21), logit (22), and probit (23):

$$g_{t,p} = \exp(7s_{t,p}) \quad (18)$$

$$g_{t,p} = \frac{1}{1 + \exp(-7s_{t,p})} \quad (19)$$

$$g_{t,p} = 1 + \tanh(7s_{t,p}) \quad (20)$$

$$g_{t,p} = 1/7 + 7s_{t,p}\mathbb{I}\{s_{t,p} \geq 0\} - 7s_{t,p}\mathbb{I}\{s_{t,p} < 0\} \quad (21)$$

$$g_{t,p} = \max\left(0, \text{logit}\left(\frac{1 + s_{t,p}}{2}\right)\right) \quad (22)$$

$$g_{t,p} = \max\left(0, \Phi^{-1}\left(\frac{1 + s_{t,p}}{2}\right)\right) \quad (23)$$

$$\pi_{t,p} = \frac{g_{t,p}}{\|\mathbf{g}_t\|_1}$$

where  $\Phi^{-1}(\cdot)$  is the PPF of standard Gaussian distribution. All of the above  $\pi_{t,p}$  are bounded inside  $[0, 1]$  and give higher values to those with higher similarities.

### 3.3. Blending or switching: to randomize or to maximize

In the third step, portfolios with higher recent optimality among peers  $\pi_p$  are assigned higher action preferences  $\psi_p$ . As the agent's policy model, we fit distributions for  $\pi_p$ , to estimate their parameters  $\theta_p$  and calculate the blending ratio  $\psi_p$ .

#### 3.3.1. Blending

Portfolio blending is achieved through a probabilistic approach known as probability-matching or Herrnstein's law (Lo et al., 2021), where we estimate the parameters  $\theta \in \mathbb{R}^{1 \times P}$  by assuming multivariate distributions for  $\pi$  and then allocate fractional blending weights  $\psi_p \in (0, 1)$  proportional to  $\mathbb{E}[\pi_p|\theta]$ :

$$\psi_p = \frac{\mathbb{E}[\pi_p|\theta]}{\sum_p \mathbb{E}[\pi_p|\theta]}$$

For  $\pi_p$  generated from the maxout activation function, we fit the categorical distribution,  $\text{Cat}(\theta_1, \dots, \theta_p, \dots, \theta_P)$  using weighted maximum likelihood estimation (WMLE):

$$\begin{aligned}
\hat{\theta} &= \arg \max \sum_p \sum_t \gamma^t \mathcal{L}(\theta_p | \pi_{t,p}) \\
&= \arg \max \sum_p \sum_t \gamma^t \pi_{t,p} \log(\theta_p) \\
&\text{s.t. } \|\theta\|_1 = 1, \theta_p > 0 \\
\hat{\theta}_p &= \frac{\sum_t \gamma^t \pi_{t,p}}{\sum_p \sum_t \gamma^t \pi_{t,p}}
\end{aligned}$$

where the sum is over the previous  $t$  steps in the rolling window and the portfolios are indexed by  $p$ .  $\gamma \in (0, 1)$  is the decay factor that places more weight on recent performances, and  $\hat{\theta}_p$  is the parameter estimate of  $\pi_p$  after reviewing a rolling window.

For  $\pi_p$  generated from other activation functions, we fit the Dirichlet distribution,  $\text{Dir}(\theta_1, \dots, \theta_p, \dots, \theta_P)$  using WMLE:

$$\begin{aligned}
\hat{\theta} &= \arg \max \sum_t \gamma^t \mathcal{L}(\theta_p | \pi_{t,p}) \\
&= \arg \max \sum_t \gamma^t \log \left[ \frac{\Gamma(\sum_p \theta_p)}{\prod_p \Gamma(\theta_p)} \prod_p \pi_{t,p}^{\theta_p - 1} \right] \\
&\text{s.t. } \theta_p > 0
\end{aligned}$$

where  $\Gamma(\cdot)$  is the gamma function.

For both the categorical distribution and Dirichlet distribution, we have  $\mathbb{E}[\pi_p | \theta_p] = \theta_p$ . Thus, the blending ratio vector  $\psi$  and the parameter estimates vector  $\hat{\theta}$  are aligned,

$$\hat{\psi}_p = \frac{\hat{\theta}_p}{\sum_p \hat{\theta}_p}$$

Note the probability-matching strategy can also be conceptualized as maximizing the projection from the 2-norm re-scaled blending ratio vector  $\psi$  onto the parameter estimates vector  $\hat{\theta}$ .



$$\begin{aligned}
\hat{\psi} &= \arg \max \cos(\psi, \hat{\theta}) \\
&= \arg \max \frac{\psi}{\|\psi\|_2} \cdot \hat{\theta} \\
&s.t. \|\psi\|_1 = 1, \psi_p > 0
\end{aligned}$$

### 3.3.2. Switching

Portfolio switching, as a special case of blending, restricts binary  $\psi_p \in \{0, 1\}$ , indicating that investors hold strong positive beliefs and invest entirely in the arm with the highest  $\theta_p$ . Switching is often rationalized in high-conviction investment scenarios, reflecting the belief that “wide diversification is only required when investors do not understand what they are doing”. In the case of portfolio switching,  $\pi_p$  can be modeled as a univariate random variable for each  $p$ .

For  $\pi_p$  generated from the maxout activation function, we fit a Bernoulli distribution,  $\text{Bernoulli}(\theta_p)$  for each portfolio  $p$  using WMLE:

$$\begin{aligned}
\hat{\theta} &= \arg \max \sum_p \sum_t \gamma^t \mathcal{L}(\theta_p | \pi_{t,p}) \\
\hat{\theta}_p &= \arg \max \sum_t \gamma^t \left( \pi_{t,p} \log \theta_p + (1 - \pi_{t,p}) \log(1 - \theta_p) \right) \\
&s.t. \theta_p \in (0, 1) \\
\hat{\theta}_p &= \frac{\sum_t \gamma^t \pi_{t,p}}{\sum_t (\gamma^t \pi_{t,p} + \gamma^t (1 - \pi_{t,p}))} = \frac{\sum_t \gamma^t \pi_{t,p}}{\sum_t \gamma^t}
\end{aligned}$$

For  $\pi_p$  generated from other activation functions, we fit a beta distribution,  $\text{Beta}(\theta_p, \nu_p)$  for each portfolio  $p$  using WMLE:

$$\begin{aligned}
\hat{\theta} &= \arg \max \sum_p \sum_t \gamma^t \mathcal{L}(\theta_p | \pi_{t,p}) \\
\hat{\theta}_p &= \arg \max \sum_t \gamma^t \left( (\theta_p \nu_p - 1) \log(\pi_{t,p}) + (\nu_p - \theta_p \nu_p - 1) \log(1 - \pi_{t,p}) \right. \\
&\quad \left. - \log \mathcal{B}(\theta_p \nu_p, \nu_p - \theta_p \nu_p) \right) \\
&s.t. \theta_p \in (0, 1)
\end{aligned}$$

where  $\mathcal{B}(\cdot, \cdot)$  is the beta function.

For Bernoulli distribution and beta distribution, we have  $\mathbb{E}[\pi_p|\theta_p] = \theta_p$ . The portfolio switching strategy can be conceptualized as maximizing the projection from the raw blending ratio vector  $\psi$  onto the parameter estimates vector  $\hat{\theta}$ :

$$\begin{aligned} \hat{\psi} &= \arg \max \psi \cdot \hat{\theta} \\ s.t. \quad &\|\psi\|_1 = 1, \psi_p > 0 \\ \hat{\psi}_p &= \mathbb{I}\{p = \arg \max_q \hat{\theta}_q\} \end{aligned}$$

### 3.4. Backtest

To backtest eclectic portfolios, we retrieved price time series from Coinbase (we use a different exchange for this backtest, just to be sure our results are not sensitive to the data sources), spanning from 2019-08-08 to 2023-08-17, covering 10 currencies priced in USD including BCH, BTC, EOS, ETC, ETH, LINK, LTC, XLM, XTZ, and ZRX. As depicted in fig. 5, asset returns have notable high correlations. Rebalancing occurs every two days. At every step, we solve optimal portfolio weights  $\mathbf{w}_{0,p}$  of each arm according to different generative model forecasts and proxy objective functions. We then calculate optimal blending ratios  $\psi$  according to different similarity functions  $s_p$ , activation functions  $\pi_p$ , decay factors  $\gamma \in \{0.9, 0.99, 0.999\}$ , and blending methods (blending or switching). The rolling window length of historical asset returns for generative model fitting is 91 steps or 182 days. The rolling window length of historical  $\pi_p$  for  $\theta_p$  estimation and  $\psi$  calculation is 26 steps or 52 days. The transaction cost  $c$  is set as 50 bps, together with the number of assets  $D = 10$  and the constraint boundary multiplier  $m = 5$ . To ensure robustness and assess performance consistency, we conduct multiple independent simulations using different random seeds. In total, we have 5460 paths and each has 619 steps.

For performance attribution, we fit LASSO (14) to eclectic portfolio performances per step, similar to what we have done for evaluating diverse pairings of generative model forecasts and objective functions used for portfolio optimization in the previous section. We use the eclectic portfolio simple return  $r_p$  (15) and the logit of cosine similarity between eclectic portfolio weights

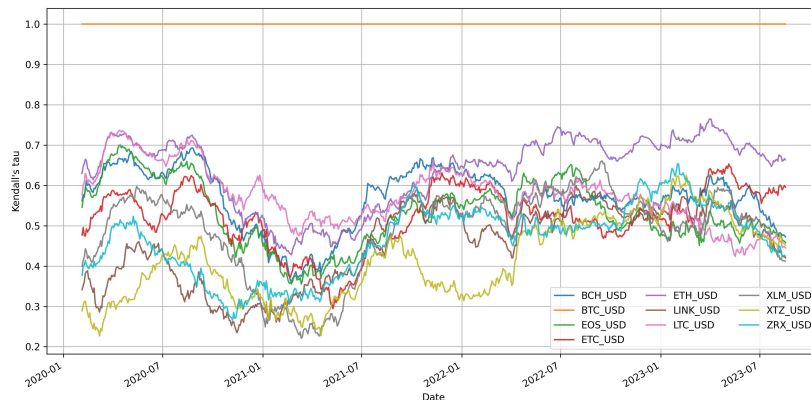


Figure 5: Kendall’s  $\tau$  between BTC and studied crypto-currencies, using a 182-day rolling window of 2-day simple returns as priced in USD on Coinbase.

and asset returns (16) as the performance measure  $y$ . The design matrix  $\mathbf{X} \in \mathbb{R}^{3379740 \times 119}$  is filled with binary values (0 or 1) encoding the presence of the foundation elements used in the eclectic portfolio construction: intercept, various similarity functions, optimality activation functions, decay factors, blending methods, and their two-variable interaction terms. While  $\mathbf{X}$  has 119 columns, each row contains only eleven instances of the value 1. The performance measures, represented as the column vector  $\mathbf{y} \in \mathbb{R}^{3379740 \times 1}$  encompass data from all steps in all simulation paths. The optimal  $\lambda^*$  is selected based on 7-fold CV that minimizes MSE.

We present the non-zero coefficients obtained at the optimal  $\lambda^*$  in LASSO models for the  $r_p$  in table 3 and for the logit-cosine performance measure in table 4. The significance of interaction terms between similarities and activation functions are apparent with their positive coefficients persisting in LASSO model. The coefficients for the value models are of larger magnitude compared to those for the policy models; this indicates a good value model outweighs action selection policies. The specific value model combination of using cosine for similarity and logit activation function for optimality has the biggest coefficient in LASSO model for performance attribution. This combination also leads to the best performing eclectic portfolio as shown in fig. 6d. However, the group average using logit activation function alone, does not stand out as shown in fig. 6b. In general, most group-average logit-cosine performance measures exhibit negative trends. Furthermore, in fig. 6c,

we see that portfolios with a decay factor  $\gamma = 0.999$  showed better performances than those with smaller  $\gamma$ . A larger  $\gamma$  lets more historical  $\pi_p$  records effectively engage in the WMLE of  $\hat{\theta}_p$  and the policy model of  $\psi$ . Though a shorter lookback window may lead to a swifter adaptation of the policy model, for this market a larger sample size is beneficial.

Table 3: Non-zero coefficients in LASSO for eclectic portfolio simple return, corresponding to combinations of similarities, activation functions, decay factors, and blending methods.

coefficient	value
intercept	0.052420
SimiMtd cosine : ActFun logit	0.040435
SimiMtd L1 : ActFun probit	0.032191
SimiMtd ndtr : ActFun softmax	0.029074
SimiMtd ndtr : ActFun logistic	0.021552
SimiMtd ndtr : ActFun tanh	0.021014
ActFun logistic	0.018417
ActFun leaky relu	0.016727
SimiMtd Linf : ActFun maxout	0.015468
SimiMtd L2 : ActFun leaky relu	0.013818
SimiMtd cosine : ActFun logit	0.012790
SimiMtd Linf : ActFun leaky relu	0.012582
ActFun logit	0.011888
SimiMtd L2 : ActFun tanh	0.008916
SimiMtd L2	0.008098
ActFun maxout	0.005346
SimiMtd L1 : ActFun maxout	0.002466
SimiMtd cosine : ActFun logistic	0.001398
SimiMtd L2 : ActFun softmax	0.001231
SimiMtd Linf : ActFun tanh	0.000469
SimiMtd L1	0.000295
Decay 0.999	0.000245
BldMtd switch	0.000034
Decay 0.9	-0.000085
SimiMtd Linf	-0.001580
SimiMtd cosine	-0.001636
SimiMtd Linf : ActFun probit	-0.001769
SimiMtd L2 : ActFun maxout	-0.006973
SimiMtd L1 : ActFun tanh	-0.008966
SimiMtd L1 : ActFun leaky relu	-0.014248
ActFun probit	-0.016101
SimiMtd L1 : ActFun softmax	-0.016573
SimiMtd ndtr : ActFun probit	-0.017719
SimiMtd L2 : ActFun logit	-0.028180
SimiMtd Linf : ActFun logit	-0.028317
SimiMtd ndtr : ActFun logit	-0.045055

To provide a concrete example of the best-performing candidate identified through LASSO results, we present the backtest performances of portfolios using cosine for similarity and logit for optimality with a decay factor

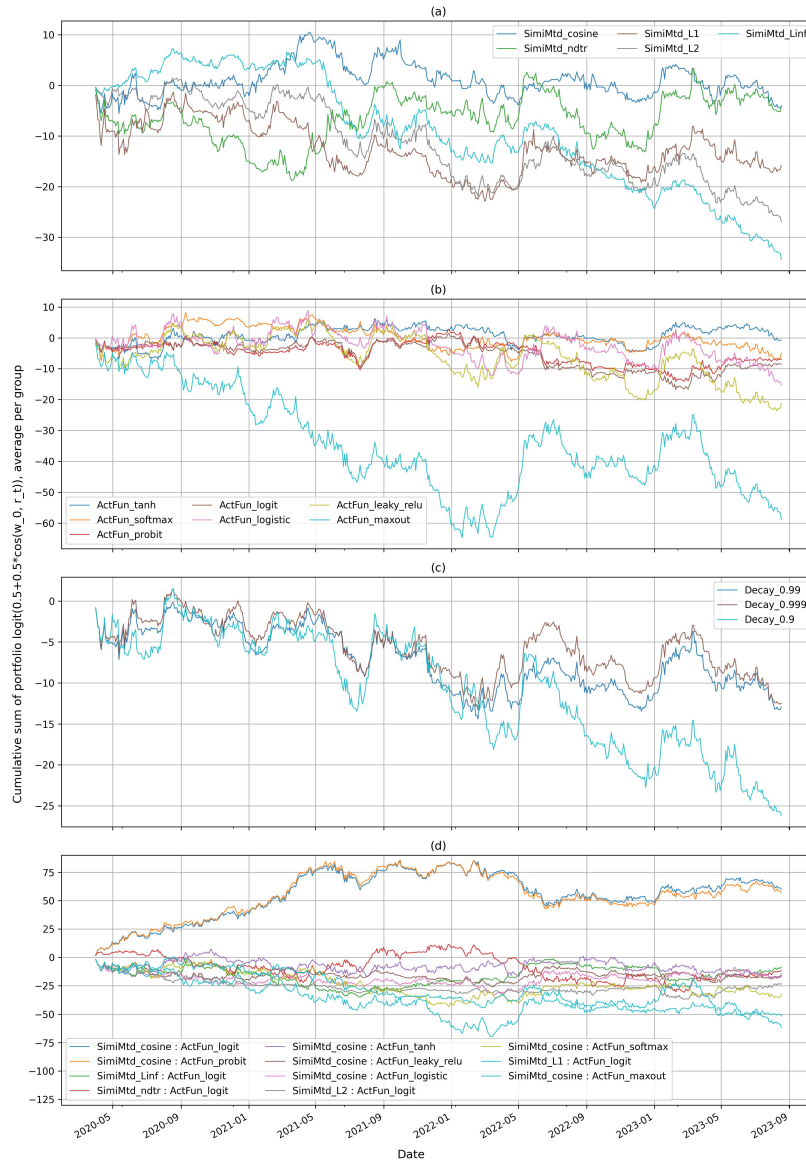


Figure 6: Cumulative sum of logit-cosine performance measure, averaged for eclectic portfolios as grouped by (a) similarity, (b) activation function, (c) decay factor, and (d) combination of similarity and activation function that use either cosine similarity or logit activation function.

Table 4: Non-zero coefficients in LASSO for eclectic portfolio logit-cosine performance measure, corresponding to combinations of similarities, activation functions, decay factors, and blending methods.

coefficient	value
SimiMtd cosine : ActFun logit	0.694396
SimiMtd cosine : ActFun probit	0.683284
SimiMtd ndtr : ActFun softmax	0.629263
SimiMtd L1 : ActFun logit	0.583020
SimiMtd L1 : ActFun probit	0.574046
ActFun logistic	0.518490
SimiMtd Linf : ActFun leaky relu	0.387092
ActFun leaky relu	0.355478
SimiMtd ndtr : ActFun tanh	0.346860
ActFun maxout	0.276777
SimiMtd L2 : ActFun tanh	0.274927
SimiMtd Linf : ActFun maxout	0.264649
intercept	0.235726
SimiMtd L2 : ActFun leaky relu	0.183136
SimiMtd L2	0.159240
SimiMtd ndtr : ActFun logistic	0.141152
Decay 0.999	0.111536
SimiMtd ndtr	0.076147
Decay 0.99	0.043022
SimiMtd ndtr : ActFun maxout	0.039835
SimiMtd L2 : ActFun softmax	0.004616
BldMtd switch	0.002090
SimiMtd L1 : ActFun softmax	-0.016793
SimiMtd cosine	-0.030179
ActFun logit	-0.042316
SimiMtd L2 : ActFun maxout	-0.112805
ActFun softmax	-0.125102
SimiMtd cosine : ActFun tanh	-0.176605
SimiMtd Linf : ActFun softmax	-0.217533
SimiMtd ndtr : ActFun leaky relu	-0.259776
SimiMtd L2 : ActFun logit	-0.378502
SimiMtd L2 : ActFun probit	-0.411934
SimiMtd Linf : ActFun logit	-0.533289
SimiMtd Linf : ActFun probit	-0.651316
SimiMtd ndtr : ActFun logit	-1.109325
SimiMtd ndtr : ActFun probit	-1.150317

$\gamma = 0.999$  in fig. 7. It can be seen from the figure that all simulated paths consistently outperform the benchmark, which maintains long-weight parity but without including transaction costs in portfolio return. This figure also shows that the level of outperformance achieved by the eclectic portfolio to its benchmark significantly surpasses the outperformance achieved by any individual generative model-based portfolios to their benchmarks shown in fig. 4.

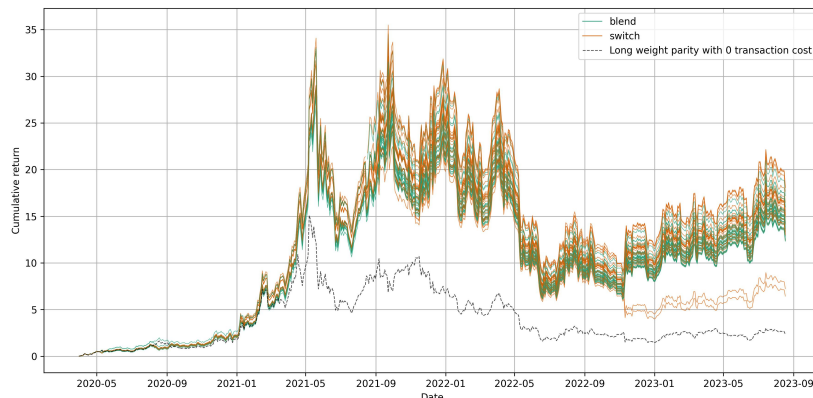


Figure 7: Visualization of eclectic portfolios using cosine similarity function and logit activation function with a decay factor  $\gamma = 0.999$ , in cumulative simple returns.

For portfolio groups using blending or switching, we chart the averaged final portfolio weights  $\mathbf{w}_0$  and blending ratio  $\psi$  in fig. 8. We also plot their group averaged cumulative sum of the logit-cosine performance measure and the logit-turnover in fig. 9, where the logit-turnover eq. (24) is defined as:

$$\text{logit} \left( \frac{\|\mathbf{w}_{t,0} - \mathbf{w}_{t-1,1}\|_1}{2} \right) \quad (24)$$

As evident in fig. 8, switching portfolios have more concentrated blending ratios  $\psi$  than blending portfolios, and their asset weights  $\mathbf{w}_0$  display a similar pattern. Both policy models allow for abrupt  $\psi$  evolution and occasionally all-in short-weight parity portfolios, which is not common in traditional portfolio theory. It can be seen from fig. 9, switching portfolios have less turnover, higher  $r_p$ , and higher logit-cosine performance measure.

#### 4. Conclusion and future research

In this paper, we embark on a comprehensive exploration of our portfolio construction framework, delving into its foundation elements and conducting a thorough evaluation of its efficacy. Operating within the dynamic and evolving realm of cryptocurrencies, we craft a portfolio framework that is not only applicable to the cryptocurrency domain but also relevant to broader financial markets.

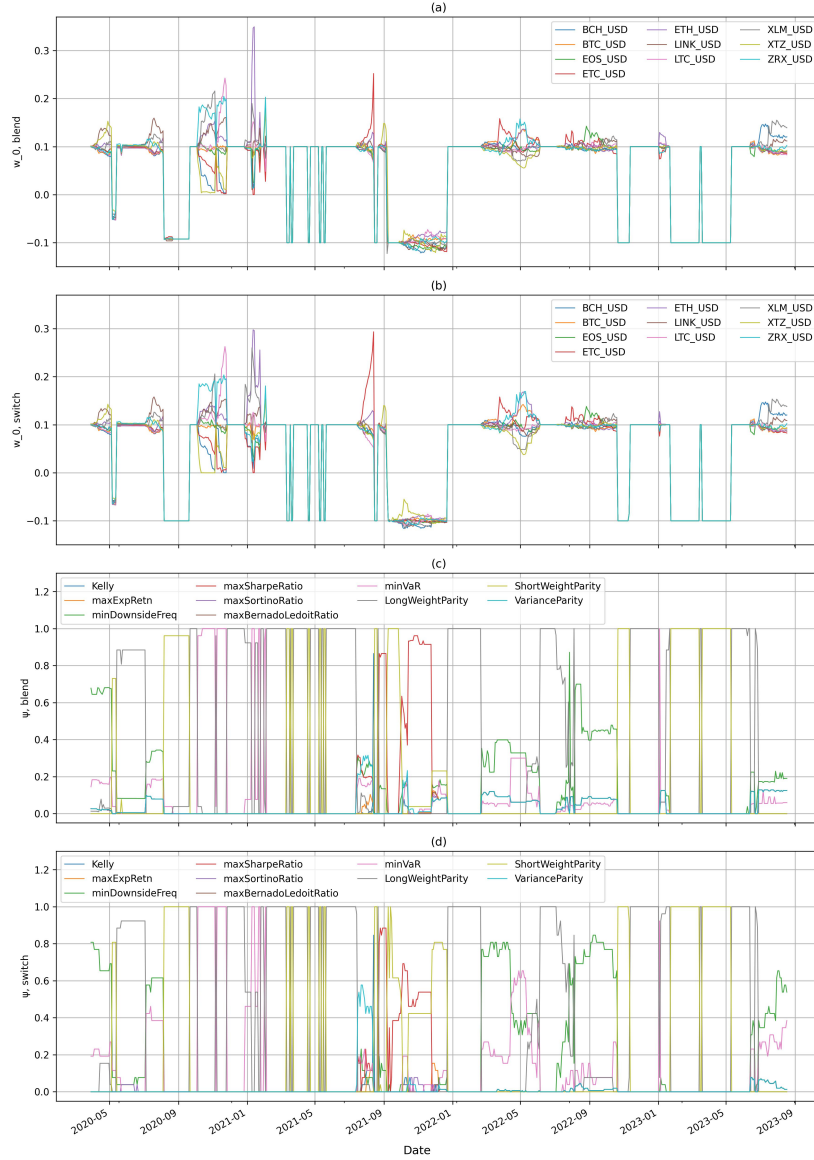


Figure 8: (a) Asset weights  $\mathbf{w}_0$  for blending portfolios, (b) asset weights  $\mathbf{w}_0$  for switching portfolios, (c) blending ratio  $\psi$  for blending portfolios, and (d) blending ratio  $\psi$  for switching portfolios. All in group average from eclectic portfolios using cosine similarity function and logit activation function with a decay factor  $\gamma = 0.999$ .



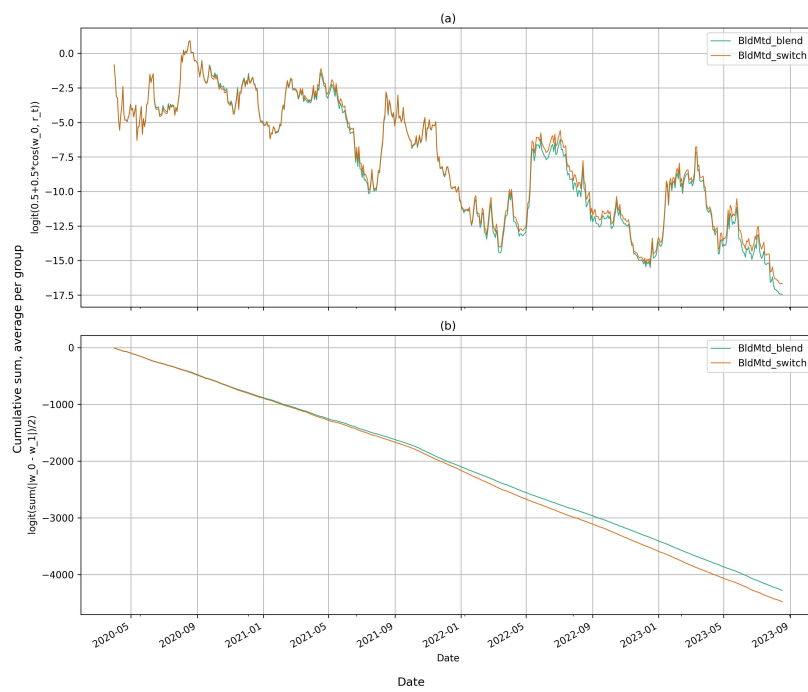


Figure 9: Cumulative sum of (a) logit-cosine performance measure and (b) logit-turnover, in group average from all eclectic portfolios.

Leveraging high-performance computing, we meticulously investigated diverse pairings of generative model forecasts and proxy objective functions. Our findings underscored the pivotal role played by proxy objective functions, as evidenced by their larger coefficient in performance LASSO models. Notably, the vine copula emerged as a superior choice for multivariate dependence modeling, and Sharpe ratio portfolios consistently outperformed alternative approaches.

To align with a broad spectrum of investment strategies, we introduced eclectic portfolios, by extending the multi-armed bandit framework to portfolio blending. This approach blends optimal weights from different portfolios in a long-only manner, promoting diversification and leveraging historical feedback for refinement. We introduced similarity and optimality measures for value models and then employed probability-matching (“blending”) and a greedy algorithm (“switching”) for policy models. Notably, the specific value model using cosine similarity and logit activation function for optimality consistently delivered robust coefficients in the LASSO analysis. Switching portfolios exhibited higher variability but also achieved superior average performance compared to blending portfolios. The extent of outperformance by eclectic portfolios over their benchmarks significantly surpassed that achieved by individual generative model-based portfolios over their respective benchmarks.

In summary, our exploration of generative model-based cryptocurrency portfolios illustrates the potential for portfolio diversification and optimization through our framework. The versatility of this approach, coupled with its capacity to leverage historical full feedback, positions eclectic portfolios as an attractive option for portfolio strategies.

Looking ahead to future research, we envision the expansion of this framework to encompass various decision processes, including causal decision theory and Delphi methods (Dalkey and Helmer, 1963). The framework can be extended to incorporate proprietary alpha models into returns matrix  $R^{\mathbb{P}}$  for portfolio construction (Garthwaite and Dickey, 1996). Further investigation into proxy objective functions tailored to address tail risks with a Pareto distribution assumption (Chen and Cheng, 2022) could provide valuable insights into the widely recognized “lollapalooza” effect. The policy model,

which relies on binomial, categorical, and beta distributions can benefit from conjugate priors and Bayesian learning. In addition, different investment mandates such as those centered on ESG or CSR are existing candidates to blend for ethical and sustainability objectives. Furthermore, addressing multi-step asset return forecasts and solving multi-step portfolio optimization (1), potentially utilizing dynamic programming (Isichenko, 2021), represents both an opportunity and a computational challenge.

### Acknowledgment

We thank Mr. Linghao Huang for his help in validating the DCC-GARCH model as well as Mr. Kaihao Chen and Mr. Xuxin Gao for their help in validating backtest processes. We appreciate the two anonymous reviewers for their constructive comments and inspiring questions.

### References

- Acerbi, C., 2002. Spectral measures of risk: A coherent representation of subjective risk aversion. *Journal of Banking & Finance* 26, 1505–1518. doi:[https://doi.org/10.1016/S0378-4266\(02\)00281-9](https://doi.org/10.1016/S0378-4266(02)00281-9).
- Akaike, H., 1998. Information theory and an extension of the maximum likelihood principle, in: Parzen, E., Tanabe, K., Kitagawa, G. (Eds.), *Selected Papers of Hirotugu Akaike*. Springer New York, New York, NY, pp. 199–213. doi:[10.1007/978-1-4612-1694-0\\_15](https://doi.org/10.1007/978-1-4612-1694-0_15).
- Bernardo, A.E., Ledoit, O., 2000. Gain, loss, and asset pricing. *Journal of Political Economy* 108, 144–172. doi:[10.1086/262114](https://doi.org/10.1086/262114).
- Bollerslev, T., 1986. Generalized autoregressive conditional heteroskedasticity. *Journal of Econometrics* 31, 307–327. doi:[https://doi.org/10.1016/0304-4076\(86\)90063-1](https://doi.org/10.1016/0304-4076(86)90063-1).
- Chen, K., Cheng, T., 2022. Measuring tail risks. *The Journal of Finance and Data Science* 8, 296–308. doi:[10.1016/j.jfds.2022.11.001](https://doi.org/10.1016/j.jfds.2022.11.001).
- Czado, C., 2019. Analyzing dependent data with vine copulas: A practical guide with R. *Lecture Notes in Statistics*, Springer 222. doi:<https://doi.org/10.1007/978-3-030-13785-4>.

- Czado, C., Bax, K., Sahin, Ö., Nagler, T., Min, A., Paterlini, S., 2022. Vine copula based dependence modeling in sustainable finance. *The Journal of Finance and Data Science* 8, 309–330. doi:<https://doi.org/10.1016/j.jfds.2022.11.003>.
- Dalkey, N., Helmer, O., 1963. An experimental application of the delphi method to the use of experts. *Management science* 9, 458–467.
- De Prado, M.L., 2018. The 10 reasons most machine learning funds fail. *The Journal of Portfolio Management* 44, 120–133. doi:[10.3905/jpm.2018.44.6.120](https://doi.org/10.3905/jpm.2018.44.6.120).
- Dißmann, J., Brechmann, E.C., Czado, C., Kurowicka, D., 2013. Selecting and estimating regular vine copulae and application to financial returns. *Computational Statistics & Data Analysis* 59, 52–69. doi:<https://doi.org/10.1016/j.csda.2012.08.010>.
- Efron, B., Hastie, T., Johnstone, I., Tibshirani, R., 2004. Least angle regression. *The Annals of Statistics* 32, 407 – 499. doi:[10.1214/009053604000000067](https://doi.org/10.1214/009053604000000067).
- Engle, R., 2002. Dynamic conditional correlation: A simple class of multivariate generalized autoregressive conditional heteroskedasticity models. *Journal of Business & Economic Statistics* 20, 339–350. URL: <http://www.jstor.org/stable/1392121>.
- Fernholz, R., 1999. On the diversity of equity markets. *Journal of Mathematical Economics* 31, 393–417. doi:[https://doi.org/10.1016/S0304-4068\(97\)00018-9](https://doi.org/10.1016/S0304-4068(97)00018-9).
- Friedman, M., Savage, L.J., 1948. The utility analysis of choices involving risk. *Journal of Political Economy* 56, 279–304. URL: <http://www.jstor.org/stable/1826045>.
- Fujishima, K., Nakagawa, K., 2022. Multiple portfolio blending strategy with thompson sampling, in: 2022 12th International Congress on Advanced Applied Informatics (IIAI-AAI), IEEE. pp. 449–454.
- Garthwaite, P.H., Dickey, J.M., 1996. Quantifying and using expert opinion for variable-selection problems in regression. *Chemometrics and Intelligent Laboratory Systems* 35, 1–26. doi:[https://doi.org/10.1016/S0169-7439\(96\)00035-4](https://doi.org/10.1016/S0169-7439(96)00035-4).

- Heckerman, D., Shachter, R., 1995. Decision-theoretic foundations for causal reasoning. *J. Artif. Int. Res.* 3, 405–430.
- Howard, R.A., Matheson, J.E., North, D.W., 1972. The decision to seed hurricanes. *Science* 176, 1191–1202. doi:[10.1126/science.176.4040.1191](https://doi.org/10.1126/science.176.4040.1191).
- Isichenko, M., 2021. *Quantitative Portfolio Management: The Art and Science of Statistical Arbitrage*. Wiley.
- Joe, H., 2014. *Dependence Modeling with Copulas*. Chapman & Hall/CRC Monographs on Statistics & Applied Probability, Taylor & Francis.
- Kahneman, D., Tversky, A., 1979. Prospect Theory: An Analysis of Decision under Risk. *Econometrica* 47, 263–291. URL: <http://www.jstor.org/stable/1914185>.
- Karatzas, I., Fernholz, R., 2009. Stochastic portfolio theory: An overview, in: Bensoussan, A., Zhang, Q. (Eds.), *Special Volume: Mathematical Modeling and Numerical Methods in Finance*. Elsevier. volume 15 of *Handbook of Numerical Analysis*, pp. 89–167. doi:[https://doi.org/10.1016/S1570-8659\(08\)00003-3](https://doi.org/10.1016/S1570-8659(08)00003-3).
- Kelly Jr., J.L., 1956. A new interpretation of information rate. *Bell System Technical Journal* 35, 917–926. doi:<https://doi.org/10.1002/j.1538-7305.1956.tb03809.x>.
- Kolm, P.N., Ritter, G., Simonian, J., 2021. Black–litterman and beyond: The bayesian paradigm in investment management. *The Journal of Portfolio Management* 47, 91–113.
- Kolm, P.N., Tütüncü, R., Fabozzi, F.J., 2014. 60 years of portfolio optimization: Practical challenges and current trends. *European Journal of Operational Research* 234, 356–371. doi:<https://doi.org/10.1016/j.ejor.2013.10.060>.
- Lewis, D., 1981. Causal decision theory. *Australasian Journal of Philosophy* 59, 5–30. doi:[10.1080/00048408112340011](https://doi.org/10.1080/00048408112340011).
- Lezmi, E., Roncalli, T., Xu, J., 2022. Multi-period portfolio optimization. Available at SSRN .

- Lo, A.W., 2017. Adaptive markets: Financial evolution at the speed of thought. Princeton University Press. URL: <http://www.jstor.org/stable/j.ctvc7778k>.
- Lo, A.W., Foerster, S.R., 2021. In pursuit of the perfect portfolio. Princeton University Press, Princeton. doi:<https://doi.org/10.1515/9780691222684>.
- Lo, A.W., Marlowe, K.P., Zhang, R., 2021. To maximize or randomize? an experimental study of probability matching in financial decision making. PLOS ONE 16, 1–20. doi:[10.1371/journal.pone.0252540](https://doi.org/10.1371/journal.pone.0252540).
- Longerstae, J., Spencer, M., 1996. Riskmetrics—technical document. Morgan Guaranty Trust Company of New York: New York 51, 54.
- Malevergne, Y., Sornette, D., 2005. Higher-moment portfolio theory. The Journal of Portfolio Management 31, 49–55. doi:<https://doi.org/10.3905/jpm.2005.570150>.
- Markowitz, H., 1952. Portfolio selection. The Journal of Finance 7, 77–91. doi:<https://doi.org/10.1111/j.1540-6261.1952.tb01525.x>.
- Markowitz, H., 2006. de Finetti scoops Markowitz. Journal of Investment Management 4.
- Markowitz, H., 2014. Mean–variance approximations to expected utility. European Journal of Operational Research 234, 346–355. doi:<https://doi.org/10.1016/j.ejor.2012.08.023>.
- Markowitz, H.M., 1999. The early history of portfolio theory: 1600-1960. Financial Analysts Journal 55, 5–16. URL: <http://www.jstor.org/stable/4480178>.
- Markowitz, H.M., 2010. Portfolio theory: As I still see it. Annu. Rev. Financ. Econ. 2, 1–23.
- McElreath, R., 2020. Statistical rethinking: A Bayesian course with examples in R and Stan. CRC press.
- Munger, C.T., Kaufman, P., 2008. Poor Charlie’s Almanack. Donning.

- von Neumann, J., Morgenstern, O., Rubinstein, A., 1944. Theory of Games and Economic Behavior (60th Anniversary Commemorative Edition). Princeton University Press. URL: <http://www.jstor.org/stable/j.ctt1r2gkx>.
- Orskaug, E., 2009. DCC-GARCH model-with various error distributions. Norwegian Computing Center, Pub. no. SAMBA/19/09, Jun .
- Paolella, M.S., Polak, P., 2018. Cobra: Copula-based portfolio optimization, in: Kreinovich, V., Sriboonchitta, S., Chakpitak, N. (Eds.), Predictive econometrics and big data, Springer International Publishing, Cham. pp. 36–77.
- Pearl, J., 1995. Causal diagrams for empirical research. *Biometrika* 82, 669–688. doi:[10.1093/biomet/82.4.669](https://doi.org/10.1093/biomet/82.4.669).
- Pedregosa, F., Varoquaux, G., Gramfort, A., Michel, V., Thirion, B., Grisel, O., Blondel, M., Prettenhofer, P., Weiss, R., Dubourg, V., Vanderplas, J., Passos, A., Cournapeau, D., Brucher, M., Perrot, M., Duchesnay, E., 2011. Scikit-learn: Machine learning in python. *J. Mach. Learn. Res.* 12, 2825–2830.
- Qian, E., 2005. On the financial interpretation of risk contribution: Risk budgets do add up. Available at SSRN 684221 .
- Qian, E., 2011. Risk parity and diversification. *The Journal of Investing* 20, 119–127.
- Ramsey, F.P., 1931. The foundations of mathematical and other logical essays. Routledge and K. Paul.
- Rockafellar, R.T., Uryasev, S., others, 2000. Optimization of conditional value-at-risk. *Journal of risk* 2, 21–42.
- Rosenblatt, M., 1952. Remarks on a multivariate transformation. *The annals of mathematical statistics* 23, 470–472.
- Roy, A.D., 1952. Safety first and the holding of assets. *Econometrica: Journal of the econometric society* , 431–449.
- Rubinstein, M., 2002. Markowitz’s ”portfolio selection”: A fifty-year retrospective. *The Journal of finance* 57, 1041–1045.

- Savage, L.J., 1951. The theory of statistical decision. *Journal of the American Statistical Association* 46, 55–67. doi:[10.1080/01621459.1951.10500768](https://doi.org/10.1080/01621459.1951.10500768).
- Schmidt, U., 2004. Alternatives to expected utility: Formal theories, in: Barberà, S., Hammond, P.J., Seidl, C. (Eds.), *Handbook of Utility Theory: Volume 2 Extensions*. Springer US, Boston, MA, pp. 757–837. doi:[10.1007/978-1-4020-7964-1\\_2](https://doi.org/10.1007/978-1-4020-7964-1_2).
- Sharpe, W.F., 1966. Mutual fund performance. *The Journal of Business* 39, 119–138. URL: <http://www.jstor.org/stable/2351741>.
- Shen, W., Wang, J., 2016. Portfolio blending via thompson sampling, in: *Proceedings of the Twenty-Fifth International Joint Conference on Artificial Intelligence*, AAAI Press. p. 1983–1989.
- Soros, G., 2013. Fallibility, reflexivity, and the human uncertainty principle. *Journal of Economic Methodology* 20, 309–329.
- Sortino, F.A., Price, L.N., 1994. Performance measurement in a downside risk framework. *the Journal of Investing* 3, 59–64. doi:<https://doi.org/10.3905/joi.3.3.59>.
- Sutton, R.S., Barto, A.G., 2018. *Reinforcement learning: An introduction*. MIT Press.
- Thompson, W.R., 1933. On the likelihood that one unknown probability exceeds another in view of the evidence of two samples. *Biometrika* 25, 285–294. URL: <http://www.jstor.org/stable/2332286>.
- Thorp, E.O., 1975. Portfolio choice and the kelly criterion, in: ZIEMBA, W., VICKSON, R. (Eds.), *Stochastic Optimization Models in Finance*. Academic Press, pp. 599–619. doi:<https://doi.org/10.1016/B978-0-12-780850-5.50051-4>.
- Weinzierl, T., 2022. The pillars of science, in: *Principles of parallel scientific computing: A first guide to numerical concepts and programming methods*. Springer Nature, pp. 3–9.
- Xidonas, P., Steuer, R., Hassapis, C., 2020. Robust portfolio optimization: a categorized bibliographic review. *Annals of Operations Research* 292, 533–552. doi:[10.1007/s10479-020-03630-8](https://doi.org/10.1007/s10479-020-03630-8).